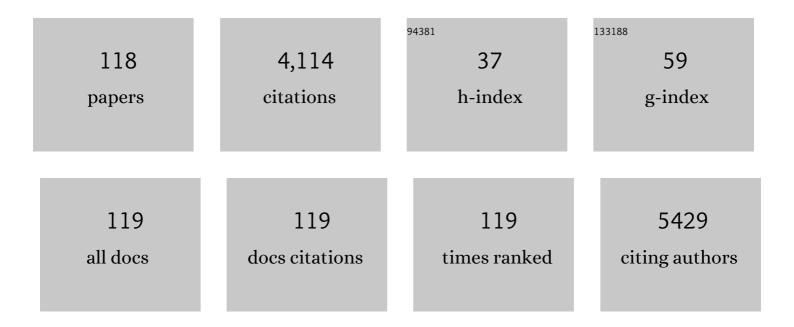
List of Publications by Year in descending order

Source: https://exaly.com/author-pdf/6811624/publications.pdf Version: 2024-02-01



#	Article	IF	CITATIONS
1	A green and easy-to-assemble electrochemical biosensor based on thylakoid membranes for photosynthetic herbicides detection. Biosensors and Bioelectronics, 2022, 198, 113838.	5.3	4
2	Correlation between impedance spectroscopy and bubble-induced mass transport in the electrochemical reduction of carbon dioxide. Journal of Energy Chemistry, 2022, 67, 500-507.	7.1	9
3	Well performing Fe-SnO2 for CO2 reduction to HCOOH. Catalysis Communications, 2022, 163, 106412.	1.6	9
4	Novel Insights into Sb-Cu Catalysts for Electrochemical Reduction of CO2. Applied Catalysis B: Environmental, 2022, 306, 121089.	10.8	25
5	Insights into the Electrochemical Reduction of 5â€Hydroxymethylfurfural at High Current Densities. ChemSusChem, 2022, 15, .	3.6	14
6	Characterization of Chemically Modified TiO ₂ Synthesized via Sustainable Superoxidation of Ti. Journal of Physical Chemistry C, 2022, 126, 6223-6230.	1.5	1
7	Microwave-Assisted Synthesis of Nitrogen and Sulphur Doped Graphene Decorated with Antimony Oxide: An Effective Catalyst for Oxygen Reduction Reaction. Materials, 2022, 15, 10.	1.3	4
8	Facile synthesis of cubic cuprous oxide for electrochemical reduction of carbon dioxide. Journal of Materials Science, 2021, 56, 1255-1271.	1.7	19
9	N-doping modification by plasma treatment in polyacrylonitrile derived carbon-based nanofibers for Oxygen Reduction Reaction. International Journal of Hydrogen Energy, 2021, 46, 13845-13854.	3.8	11
10	Biochar/Zinc Oxide Composites as Effective Catalysts for Electrochemical CO ₂ Reduction. ACS Sustainable Chemistry and Engineering, 2021, 9, 5445-5453.	3.2	46
11	Enhanced Power Extraction with Sediment Microbial Fuel Cells by Anode Alternation. Fuels, 2021, 2, 168-178.	1.3	4
12	Zn- and Ti-Doped SnO2 for Enhanced Electroreduction of Carbon Dioxide. Materials, 2021, 14, 2354.	1.3	7
13	AgCu Bimetallic Electrocatalysts for the Reduction of Biomass-Derived Compounds. ACS Applied Materials & Interfaces, 2021, 13, 23675-23688.	4.0	35
14	Polymer-metal complexes as emerging catalysts for electrochemical reduction of carbon dioxide. Journal of Applied Electrochemistry, 2021, 51, 1301-1311.	1.5	12
15	Integration of Portable Sedimentary Microbial Fuel Cells in Autonomous Underwater Vehicles. Energies, 2021, 14, 4551.	1.6	5
16	A Study of the Effect of Electrode Composition on the Electrochemical Reduction of CO2. Catalysis Today, 2021, , .	2.2	13
17	Efficient CO2 Electroreduction on Tin Modified Cuprous Oxide Synthesized via a One-Pot Microwave-Assisted Route. Catalysts, 2021, 11, 907.	1.6	2
18	Tandem devices for simultaneous CO2 reduction at the cathode and added-value products formation at the anode. Journal of CO2 Utilization, 2021, 52, 101697.	3.3	12

#	Article	IF	CITATIONS
19	Facilely synthesized nitrogen-doped reduced graphene oxide functionalized with copper ions as electrocatalyst for oxygen reduction. Npj 2D Materials and Applications, 2021, 5, .	3.9	22
20	CuZnAl-Oxide Nanopyramidal Mesoporous Materials for the Electrocatalytic CO2 Reduction to Syngas: Tuning of H2/CO Ratio. Nanomaterials, 2021, 11, 3052.	1.9	10
21	Living Bacteria Directly Embedded into Electrospun Nanofibers: Design of New Anode for Bio-Electrochemical Systems. Nanomaterials, 2021, 11, 3088.	1.9	7
22	An Electrochemical Platform for the Carbon Dioxide Capture and Conversion to Syngas. Energies, 2021, 14, 7869.	1.6	5
23	Syngas production by electrocatalytic reduction of CO2 using Ag-decorated TiO2 nanotubes. International Journal of Hydrogen Energy, 2020, 45, 26458-26471.	3.8	42
24	Environmental electroactive consortia as reusable biosensing element for freshwater toxicity monitoring. New Biotechnology, 2020, 55, 36-45.	2.4	19
25	Microwaveâ€Assisted Synthesis of Copperâ€Based Electrocatalysts for Converting Carbon Dioxide to Tunable Syngas. ChemElectroChem, 2020, 7, 229-238.	1.7	22
26	An Integrated Device for the Solar-Driven Electrochemical Conversion of CO ₂ to CO. ACS Sustainable Chemistry and Engineering, 2020, 8, 7563-7568.	3.2	22
27	Coupled Copper–Zinc Catalysts for Electrochemical Reduction of Carbon Dioxide. ChemSusChem, 2020, 13, 4128-4139.	3.6	51
28	Electrospun Nanofibers: from Food to Energy by Engineered Electrodes in Microbial Fuel Cells. Nanomaterials, 2020, 10, 523.	1.9	21
29	Nonwoven mats of N-doped carbon nanofibers as high-performing anodes in microbial fuel cells. Materials Today Energy, 2020, 16, 100385.	2.5	20
30	Anodic microbial community analysis of microbial fuel cells based on enriched inoculum from freshwater sediment. Bioprocess and Biosystems Engineering, 2019, 42, 697-709.	1.7	11
31	Biohybrid Cathode in Single Chamber Microbial Fuel Cell. Nanomaterials, 2019, 9, 36.	1.9	14
32	Proving the existence of Mn porphyrin-like complexes hosted in reduced graphene oxide with outstanding performance as oxygen reduction reaction catalysts. 2D Materials, 2019, 6, 045001.	2.0	19
33	Chainlike Mesoporous SnO ₂ as a Well-Performing Catalyst for Electrochemical CO ₂ Reduction. ACS Applied Energy Materials, 2019, 2, 3081-3091.	2.5	70
34	Multifunctional flexible membranes based on reduced graphene oxide/tin dioxide nanocomposite and cellulose fibers. Electrochimica Acta, 2019, 306, 420-426.	2.6	19
35	Modeling of gas bubble-induced mass transport in the electrochemical reduction of carbon dioxide on nanostructured electrodes. Journal of Catalysis, 2019, 372, 39-48.	3.1	24
36	Sn-Decorated Cu for Selective Electrochemical CO ₂ to CO Conversion: Precision Architecture beyond Composition Design. ACS Applied Energy Materials, 2019, 2, 867-872.	2.5	41

#	Article	IF	CITATIONS
37	MnxOy- based cathodes for oxygen reduction reaction catalysis in microbial fuel cells. International Journal of Hydrogen Energy, 2019, 44, 4432-4441.	3.8	21
38	N-doped carbon nanofibers as catalyst layer at cathode in single chamber Microbial Fuel Cells. International Journal of Hydrogen Energy, 2019, 44, 4442-4449.	3.8	36
39	Greenâ€5ynthesized Nitrogenâ€Doped Carbonâ€Based Aerogels as Environmentally Friendly Catalysts for Oxygen Reduction in Microbial Fuel Cells. Energy Technology, 2018, 6, 1052-1059.	1.8	8
40	Electrospinningâ€onâ€Electrode Assembly for Airâ€Cathodes in Microbial Fuel Cells. Advanced Materials Interfaces, 2018, 5, 1801107.	1.9	7
41	Boron/Nitrogen-Codoped Carbon Nano-Onion Electrocatalysts for the Oxygen Reduction Reaction. ACS Applied Nano Materials, 2018, 1, 5763-5773.	2.4	57
42	Advanced Cu-Sn foam for selectively converting CO2 to CO in aqueous solution. Applied Catalysis B: Environmental, 2018, 236, 475-482.	10.8	118
43	Beneficial effect of Fe addition on the catalytic activity of electrodeposited MnOx films in the water oxidation reaction. Electrochimica Acta, 2018, 284, 294-302.	2.6	13
44	Electrochemical impedance spectroscopy as a tool to investigate the electroreduction of carbon dioxide: A short review. Journal of CO2 Utilization, 2018, 27, 22-31.	3.3	49
45	In situ continuous current production from marine floating microbial fuel cells. Applied Energy, 2018, 230, 78-85.	5.1	22
46	Resistive switching and impedance properties of soft nanocomposites based on Ag nanoparticles. Applied Surface Science, 2017, 424, 352-358.	3.1	9
47	Electrochemical impedance spectroscopy: Fundamentals and application in dye-sensitized solar cells. Renewable and Sustainable Energy Reviews, 2017, 79, 814-829.	8.2	212
48	Anodically-grown TiO 2 nanotubes: Effect of the crystallization on the catalytic activity toward the oxygen reduction reaction. Applied Surface Science, 2017, 412, 447-454.	3.1	18
49	Electrochemical analysis of microbial fuel cells based on enriched biofilm communities from freshwater sediment. Electrochimica Acta, 2017, 237, 133-143.	2.6	31
50	Thermal evolution of Mn _x O _y nanofibres as catalysts for the oxygen reduction reaction. Physical Chemistry Chemical Physics, 2017, 19, 28781-28787.	1.3	13
51	Fluid Dynamic Modeling for Microbial Fuel Cell Based Biosensor Optimization. Fuel Cells, 2017, 17, 627-634.	1.5	29
52	Defining the role of nanonetting in the electrical behaviour of composite nanofiber/nets. RSC Advances, 2017, 7, 38812-38818.	1.7	8
53	Effects of pH variations on anodic marine consortia in a dual chamber microbial fuel cell. International Journal of Hydrogen Energy, 2017, 42, 1820-1829.	3.8	51
54	Nanostructured MnxOy for oxygen reduction reaction (ORR) catalysts. Applied Surface Science, 2016, 388, 631-639.	3.1	42

#	Article	IF	CITATIONS
55	Oneâ€Pot Microwaveâ€Assisted Synthesis of Reduced Graphene Oxide/Iron Oxide Nanocomposite Catalyst for the Oxygen Reduction Reaction. ChemistrySelect, 2016, 1, 3640-3646.	0.7	22
56	The active modulation of drug release by an ionic field effect transistor for an ultra-low power implantable nanofluidic system. Nanoscale, 2016, 8, 18718-18725.	2.8	35
57	Toward Totally Flexible Dye-Sensitized Solar Cells Based on Titanium Grids and Polymeric Electrolyte. IEEE Journal of Photovoltaics, 2016, 6, 498-505.	1.5	70
58	Dye-sensitized solar cell for a solar concentrator system. Solar Energy, 2016, 125, 307-313.	2.9	13
59	Dynamical analysis of microbial fuel cells based on planar and 3D-packed anodes. Chemical Engineering Journal, 2016, 288, 38-49.	6.6	29
60	Microwave-Assisted Synthesis of Reduced Graphene Oxide/SnO ₂ Nanocomposite for Oxygen Reduction Reaction in Microbial Fuel Cells. ACS Applied Materials & Interfaces, 2016, 8, 4633-4643.	4.0	103
61	Self-Organized Nano- and Microstructure of Electrochemical Materials by Design of Fabrication Approaches. , 2016, , 1033-1056.		Ο
62	Anodically Grown TiO2 Nanotube Membranes: Synthesis, Characterization, and Application in Dye-Sensitized Solar Cells. , 2016, , 1299-1325.		0
63	Nanobranched ZnO Structure: pâ€Type Doping Induces Piezoelectric Voltage Generation and Ferroelectric–Photovoltaic Effect. Advanced Materials, 2015, 27, 4218-4223.	11.1	65
64	Electrodes/Electrolyte Interfaces in the Presence of a Surfaceâ€Modified Photopolymer Electrolyte: Application in Dye‧ensitized Solar Cells. ChemPhysChem, 2015, 16, 960-969.	1.0	69
65	A long-term analysis of Pt counter electrodes for Dye-sensitized Solar Cells exploiting a microfluidic housing system. Materials Chemistry and Physics, 2015, 161, 74-83.	2.0	7
66	Comparison of photocatalytic and transport properties of TiO ₂ and ZnO nanostructures for solar-driven water splitting. Physical Chemistry Chemical Physics, 2015, 17, 7775-7786.	1.3	234
67	Photo-catalytic activity of BiVO4 thin-film electrodes for solar-driven water splitting. Applied Catalysis A: General, 2015, 504, 266-271.	2.2	58
68	Dispelling clichÃ \mathbb{O} s at the nanoscale: the true effect of polymer electrolytes on the performance of dye-sensitized solar cells. Nanoscale, 2015, 7, 12010-12017.	2.8	68
69	Electrochemical and impedance characterization of Microbial Fuel Cells based on 2D and 3D anodic electrodes working with seawater microorganisms under continuous operation. Bioresource Technology, 2015, 195, 139-146.	4.8	56
70	As-grown vertically aligned amorphous TiO2 nanotube arrays as high-rate Li-based micro-battery anodes with improved long-term performance. Electrochimica Acta, 2015, 151, 222-229.	2.6	73
71	Enhancement of photoconversion efficiency in dye-sensitized solar cells exploiting pulsed laser deposited niobium pentoxide blocking layers. Thin Solid Films, 2015, 574, 38-42.	0.8	18
72	Toward quasi-solid state Dye-sensitized Solar Cells: Effect of γ-Al 2 O 3 nanoparticle dispersion into liquid electrolyte. Solar Energy, 2015, 111, 125-134.	2.9	24

#	Article	IF	CITATIONS
73	Anodically Grown TiO2 Nanotube Membranes: Synthesis, Characterization, and Application in Dye-Sensitized Solar Cells. , 2015, , 1-23.		0
74	Impedance spectroscopy analysis of the tunnelling conduction mechanism in piezoresistive composites. Journal Physics D: Applied Physics, 2014, 47, 345306.	1.3	20
75	Coral-shaped ZnO nanostructures for dye-sensitized solar cell photoanodes. Progress in Photovoltaics: Research and Applications, 2014, 22, 189-197.	4.4	34
76	Multi-functional energy conversion and storage electrodes using flower-like Zinc oxide nanostructures. Energy, 2014, 65, 639-646.	4.5	87
77	Multifunctional NIR-reflective and self-cleaning UV-cured coating for solar cell applications based on cycloaliphatic epoxy resin. Progress in Organic Coatings, 2014, 77, 458-462.	1.9	30
78	Polymer electrolytes for dye-sensitized solar cells prepared by photopolymerization of PEG-based oligomers. International Journal of Hydrogen Energy, 2014, 39, 3036-3045.	3.8	67
79	Additives and salts for dye-sensitized solar cells electrolytes: what is the best choice?. Journal of Power Sources, 2014, 264, 333-343.	4.0	76
80	Sponge-like ZnO nanostructures by low temperature water vapor-oxidation method as dye-sensitized solar cell photoanodes. Journal of Alloys and Compounds, 2014, 615, S487-S490.	2.8	20
81	Thick mesoporous TiO 2 films through a sol–gel method involving a non-ionic surfactant: Characterization and enhanced performance for water photo-electrolysis. International Journal of Hydrogen Energy, 2014, 39, 21512-21522.	3.8	37
82	New Transparent Laser-Drilled Fluorine-doped Tin Oxide covered Quartz Electrodes for Photo-Electrochemical Water Splitting. Electrochimica Acta, 2014, 131, 184-194.	2.6	35
83	Novel spongelike nanostructured ZnO films: Properties and applications. Journal of Alloys and Compounds, 2014, 586, S331-S335.	2.8	9
84	Investigation of Transport and Recombination Properties in Graphene/Titanium Dioxide Nanocomposite for Dye-Sensitized Solar Cell Photoanodes. Electrochimica Acta, 2014, 131, 154-159.	2.6	56
85	TiO 2 nanotubes as flexible photoanode for back-illuminated dye-sensitized solar cells with hemi-squaraine organic dye and iodine-free transparent electrolyte. Organic Electronics, 2014, 15, 3715-3722.	1.4	74
86	Optimization of 1D ZnO@TiO ₂ Core–Shell Nanostructures for Enhanced Photoelectrochemical Water Splitting under Solar Light Illumination. ACS Applied Materials & Interfaces, 2014, 6, 12153-12167.	4.0	190
87	New insights in long-term photovoltaic performance characterization of cellulose-based gel electrolytes for stable dye-sensitized solar cells. Electrochimica Acta, 2014, 146, 44-51.	2.6	72
88	Novel electrode and electrolyte membranes: Towards flexible dye-sensitized solar cell combining vertically aligned TiO2 nanotube array and light-cured polymer network. Journal of Membrane Science, 2014, 470, 125-131.	4.1	71
89	A new method for studying activity and reaction kinetics of photocatalytic water oxidation systems using a bubbling reactor. Chemical Engineering Journal, 2014, 238, 17-26.	6.6	21
90	Charge transport improvement employing TiO ₂ nanotube arrays as front-side illuminated dye-sensitized solar cell photoanodes. Physical Chemistry Chemical Physics, 2013, 15, 2596-2602.	1.3	71

#	Article	IF	CITATIONS
91	Enhancement of electron lifetime in dye-sensitized solar cells using anodically grown TiO2 nanotube/nanoparticle composite photoanodes. Microelectronic Engineering, 2013, 111, 137-142.	1.1	29
92	An easy approach for the fabrication of TiO2 nanotube-based transparent photoanodes for Dye-sensitized Solar Cells. Solar Energy, 2013, 95, 90-98.	2.9	45
93	Fabrication of microstructures on different materials by diode-pumped solid state laser writing for microfluidics applications. Microsystem Technologies, 2013, 19, 1185-1194.	1.2	1
94	Photodetection and piezoelectric response from hard and flexible sponge-like ZnO-based structures. Nano Energy, 2013, 2, 1294-1302.	8.2	18
95	A Chemometric Approach for the Sensitization Procedure of ZnO Flowerlike Microstructures for Dye-Sensitized Solar Cells. ACS Applied Materials & amp; Interfaces, 2013, 5, 11288-11295.	4.0	78
96	Modeling of the dye loading time influence on the electrical impedance of a dye-sensitized solar cell. Journal of Applied Physics, 2013, 114, 094901.	1.1	6
97	Comparison of Hemi-Squaraine Sensitized TiO ₂ and ZnO Photoanodes for DSSC Applications. Journal of Physical Chemistry C, 2013, 117, 22778-22783.	1.5	30
98	Consistent static and small-signal physics-based modeling of dye-sensitized solar cells under different illumination conditions. Physical Chemistry Chemical Physics, 2013, 15, 14634.	1.3	9
99	A UV-crosslinked polymer electrolyte membrane for quasi-solid dye-sensitized solar cells with excellent efficiency and durability. Physical Chemistry Chemical Physics, 2013, 15, 3706.	1.3	82
100	Combined experimental and theoretical investigation of the hemi-squaraine/TiO2 interface for dye sensitized solar cells. Physical Chemistry Chemical Physics, 2013, 15, 7198.	1.3	31
101	Vertically aligned TiO2 nanotube array for high rate Li-based micro-battery anodes with improved durability. Electrochimica Acta, 2013, 102, 233-239.	2.6	45
102	Monitoring the dye impregnation time of nanostructured photoanodes for dye sensitized solar cells. Journal of Physics: Conference Series, 2013, 439, 012012.	0.3	8
103	Characterization of photovoltaic modules for low-power indoor application. Applied Energy, 2013, 102, 1295-1302.	5.1	77
104	First Pseudohalogen Polymer Electrolyte for Dye-Sensitized Solar Cells Promising for <i>In Situ</i> Photopolymerization. Journal of Physical Chemistry C, 2013, 117, 20421-20430.	1.5	71
105	TiO ₂ Nanotube Array as Efficient Transparent Photoanode in Dye-Sensitized Solar Cell with High Electron Lifetime. Acta Physica Polonica A, 2013, 123, 376-379.	0.2	6
106	Sponge-like Porous ZnO Photoanodes for Highly Efficient dye-sensitized Solar Cells. Acta Physica Polonica A, 2013, 123, 386-389.	0.2	1
107	Fast TiO2Sensitization Using the Semisquaric Acid as Anchoring Group. International Journal of Photoenergy, 2013, 2013, 1-8.	1.4	4
108	Electric Characterization and Modeling of Microfluidic-Based Dye-Sensitized Solar Cell. International Journal of Photoenergy, 2012, 2012, 1-11.	1.4	14

#	Article	IF	CITATIONS
109	Microfluidic housing system: a useful tool for the analysis of dye-sensitized solar cell components. Applied Physics A: Materials Science and Processing, 2012, 109, 377-383.	1.1	19
110	An easy method for the room-temperature growth of spongelike nanostructured Zn films as initial step for the fabrication of nanostructured ZnO. Thin Solid Films, 2012, 524, 107-112.	0.8	30
111	High efficiency dye-sensitized solar cells exploiting sponge-like ZnO nanostructures. Physical Chemistry Chemical Physics, 2012, 14, 16203.	1.3	75
112	Surface energy tailoring of glass by contact printed PDMS. Applied Surface Science, 2012, 258, 9427-9431.	3.1	36
113	Fabrication of microstructures on glass by imprinting in conventional furnace for lab-on-chip application. Microelectronic Engineering, 2012, 95, 90-101.	1.1	10
114	Fabrication of large-area microfluidics structures on glass by imprinting and diode-pumped solid state laser writing techniques. Microsystem Technologies, 2011, 17, 1611-1619.	1.2	6
115	Microfluidic sealing and housing system for innovative dye-sensitized solar cell architecture. Microelectronic Engineering, 2011, 88, 2308-2310.	1.1	47
116	Real-time temperature measurement during a laser annealing process featuring a microthermocouple array: Exploiting nano and micro-metrology. Microelectronic Engineering, 2011, 88, 2484-2488.	1.1	1
117	Fabrication of microstructures on nickel alloy by DPSS laser ablation technique for lab-on-chip applications. , 2010, , .		2
118	Electrochemical Reduction of CO2 With Good Efficiency on a Nanostructured Cu-Al Catalyst. Frontiers in Chemistry, 0, 10, .	1.8	4